A Quantitative Description of the E-4031-Sensitive Repolarization Current in Rabbit Ventricular Myocytes

John R. Clay,* Azieb Ogbaghebriel,‡§ Tyna Paquette,‡ Betty I. Sasyniuk,§ and Alvin Shrier‡
*Laboratory of Neurophysiology, National Institute for Neurological Disorders and Stroke, National Institutes of Health, Bethesda, Maryland 20897, USA, and ‡Departments of Physiology and §Pharmacology, McGill University, Montréal, Québec H3G 1Y6, Canada

ABSTRACT We have measured the E-4031-sensitive repolarization current (I_{Kr}) in single ventricular myocytes isolated from rabbit hearts. The primary goal of this analysis was a description of the I_{Kr} kinetic and ion transfer properties. Surprisingly, the maximum time constant of this component was 0.8 s at 33–34°C, which is significantly greater than the value of 0.18 s previously reported under similar conditions in the original measurements of I_{Kr} from guinea pig ventricular myocytes. The primary, novel feature of our analysis concerns the relationship of the bell-shaped curve that describes the voltage dependence of the kinetics and the sigmoidal curve that describes the activation of I_{Kr}. The midpoint of the latter occurred at approximately +10 mV on the voltage axis, as compared to −30 mV for the point on the voltage axis at which the maximum time constant occurred. Moreover, the voltage dependence of the kinetics was much broader than the steepness of the activation curve would predict. Taken together, these results comprise a gating current paradox that is not resolved by the incorporation of a fast inactivated state in the analysis. The fully activated current-voltage relation for I_{Kr} exhibited strong inward-going rectification, so much so that the current was essentially nil at +30 mV, even though the channel opens rapidly in this voltage range. This result is consistent with the lack of effect of E-4031 on the early part of the plateau phase of the action potential. Surprisingly, the reversal potential of I_{Kr} was ~15 mV positive to the potassium ion equilibrium potential, which indicates that this channel carries inward current during the latter part of the repolarization phase of the action potential.

INTRODUCTION

Considerable work has been carried out on the time-dependent potassium ion current, I_K, activated during the plateau phase of the cardiac action potential, beginning with the original results on multicellular preparations by Noble and Tsien (1969) and McDonald and Trautwein (1978). More recent experiments, primarily from single, isolated cardiac myocytes, have demonstrated three potassium ion currents, namely the transient outward current, I_{to} (Coraboeuf and Carmeliet, 1982; Josephson et al., 1984; Giles and van Ginneken, 1985); the slowly activating delayed rectifier, I_{Ks} (Bennett et al., 1985; Matsuura et al., 1987; Sanguinetti and Jurkiezicz, 1990); and a second delayed rectifier component that has a current-voltage relation that strongly rectifies in the inward direction, I_{Kr} (Shrier and Clay, 1986; Shibasaki, 1987; Sanguinetti and Jurkiewicz, 1990). The latter component is selectively blocked by the Class III compounds, E-4031(1-[2-(6-methyl-2-pyridyl)ethyl]-4-(4-methylsulfonylaminobenzoyl)piperidine), dofetilide, and almokalant (Follmer and Colatsky, 1990; Sanguinetti and Jurkiewicz, 1990; Jurkiewicz and Sanguinetti, 1993; Carmeliet, 1992, 1993).

Surprisingly, a quantitative description of the E-4031-sensitive component (I_{Kr}) within the context of ion channel gating models has not yet appeared. We have undertaken this analysis with rabbit ventricular myocytes, because a kinetic description of I_{Kr} in this preparation has not, as yet, been carried out. Moreover, these preparations appear to lack a significant I_{Ks} component (Carmeliet, 1992, 1993), which is an important aid to the analysis. We have found that the I_{Kr} results comprise a paradox concerning the relationship between the kinetics of this component and its activation, as described below, which places unusual constraints on potential models of this current. An additional, novel feature of our analysis concerns the I_{Kr} reversal potential, which we found to be approximately 15 mV positive to the potassium ion equilibrium potential, E_K. This result suggests that I_{Kr} actually contributes inward current during the latter part of the repolarization phase of the action potential, although the rapid deactivation kinetics of this channel for $V < -60$ mV mitigate the effect.

Our analysis may help elucidate the role of I_{Kr} in the repolarization phase of the cardiac action potential. In particular, the results given below will be relevant to the formulation of mathematical models of the action potential.

MATERIALS AND METHODS

Isolation of ventricular myocytes

Single ventricular cells from rabbit hearts were prepared using a modification of techniques described by Mitra and Morad (1985). New Zealand white rabbits weighing 1.7–2.5 kg were anesthetized with a combination of ketamine (50 mg/kg) and xylazine (7 mg/kg) and exsanguinated via the carotid artery. The hearts were excised, mounted on a Langendorff perfusion apparatus, and perfused at 37°C with normal Tyrode's solution (see below) for 5 min followed by an additional 10 min of perfusion with nominally Ca^{2+}-free Tyrode's solution. The hearts were then perfused for 5–10 min with Ca^{2+}-free Tyrode's solution containing collagenase (type XI, 165 U/ml; Sigma Chemical Co., St. Louis, MO) followed by an

Received for publication 10 May 1995 and in final form 25 July 1995.
Address reprint requests to Dr. John R. Clay, National Institutes of Health, 36/2C02, Bethesda, MD 20892. Tel.: 301-496-7711; E-mail: jrclay@nih.gov.

0006-3495/95/11/1830/00 $2.00

additional 5–10-min perfusion with a solution containing collagenase and protease (type XIV, 0.4 U/ml; Sigma Chemical Co.). Pieces of the ventricles were then cut and placed in a K-B solution (Isenberg and Klockner, 1982) and agitated gently. The resulting single cell suspension was stored in K-B solution at room temperature. Cells were used for electrophysiological recordings within 1–8 h.

Solutions

The Tyrode's solution used in the cell isolation procedure contained (in mM): 121 NaCl, 5 KCl, 15 $NaHCO_3$, 1 Na_2HPO_4, 2.8 sodium acetate, 1 $MgCl_2$, 2.2 $CaCl_2$, and 5.5 glucose gassed with a 95% O_2/5% CO_2 mixture. The K-B solution contained (in mM): 85 KCl, 30 K_2HPO_4, 5 $MgSO_4$, 5 K_2ATP, 5 sodium pyruvate, 5 β-OH-butyric acid, 5 creatine, 20 taurine, 20 glucose, 5 sodium succinate, 0.62 polyvinylpyrolidone, and 0.5 EGTA. The pH was adjusted to 7.2 with KOH. The extracellular solution used during electrophysiological recordings contained (in mM): 121 NaCl; 2.5, 5, 10, or 15 KCl; 2.2 $CaCl_2$; 1.0 $MgCl_2$; 2.8 sodium acetate; 10 HEPES; and 10 glucose, with the pH adjusted to 7.2 by NaOH. The external solution was continuously gassed with 100% O_2. The solution in the recording pipette contained (in mM): 140 KCl, 5 ATP disodium salt, 1 $MgCl_2$, 5 HEPES, 5 EGTA, and 1.54 $CaCl_2$ with the pH adjusted to 7.0 by KOH. The calcium ion current was blocked either by nisoldipine (0.2 μM; Miles Canada Inc., Toronto) or nifedepine (5 μM, Sigma Chemical Co.). E-4031 was kindly provided by Eisai Co., Ltd. (Tsukuba Research Laboratories, Japan).

Electrical recording and data analysis

The whole cell patch clamp technique (Hamill et al., 1981) was used to record membrane currents in these experiments. Ventricular cells were placed in a chamber mounted on the stage of an inverted microscope (Zeiss IM35, OberKochen, Germany) and allowed to settle for ~5 min. The cells were continuously superfused with extracellular solution (see above) at 33–35°C. Rod-shaped myocytes with clear striations were selected for electrical recordings using an Axopatch amplifier (Axopatch-1D; Axon Instrument Corp., Foster City, CA). The pipette tip resistance was 2–4 MΩ. Voltage clamp pulses were delivered from a custom designed software package (Alembic Software Co., Montréal, Canada) implemented on a personal computer equipped with an analog-to-digital card (Omega Corp., Stamford, CT). The holding potential used throughout was −40 mV, which effectively inactivates both the sodium ion current, I_{Na}, and the transient outward current, I_{to} (Ogbaghebriel and Shrier, 1994). Membrane currents and voltages were filtered at 10 kHz, digitized at 22 kHz via a pulse code modulation unit (Neurocorder DR-390; NeuroData Corp., New York, NY), and recorded on a Betamax VCR (SL-HF 450; Sony Corp., New York, NY). Currents were analyzed off-line after filtering with a low-pass eight-pole Bessel filter at 5 kHz and digitized by a 12-bit analog-to-digital converter at 10 kHz.

RESULTS

Kinetic properties of I_K

Representative recordings of membrane current obtained in this study are illustrated in Fig. 1. The steady-state holding current at −40 mV was 0.22 nA, which is attributable to I_{K1} (Carmeliet, 1993). Moreover, −40 mV lies on the negative slope region of the I_{K1} current-voltage relation, as evidenced by the instantaneous current jumps in the inward direction, especially for the steps to −30 and −10 mV (Fig. 1). At more positive potentials, a time-independent outward current was elicited that had positive slope conductance, which may be attributable to a chloride ion component

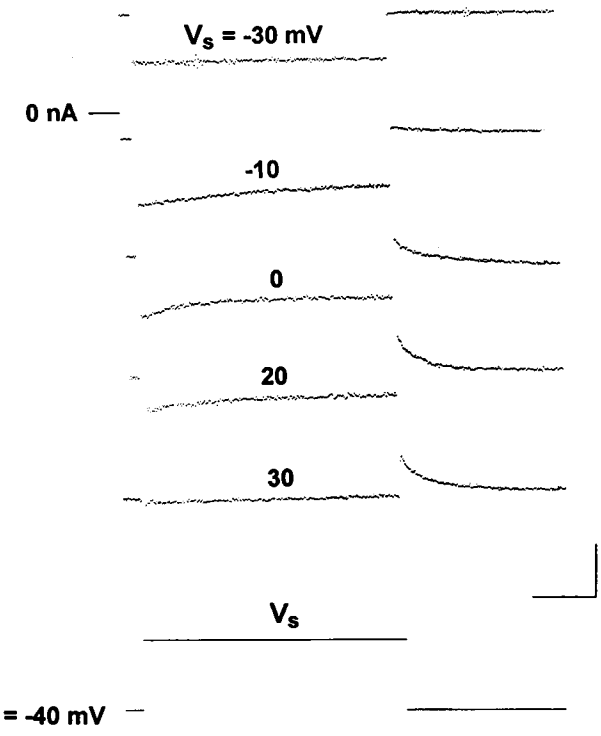

FIGURE 1 Membrane current measurements elicited by voltage steps to the potentials indicated above each record from a holding potential of −40 mV. The steady-state holding current was 0.22 nA, as indicated by the relationship between baseline current and the 0 nA mark for the −30 mV result. A similar relationship holds for the other records as well. The result for +30 mV was taken from a different preparation than the other four results. Calibrations are 0.5 s and 0.1 nA.

(Harvey and Hume, 1989; Duan et al., 1992). The latter result was quite variable from preparation to preparation. A time-dependent component (I_{Kr}) was also elicited in these experiments, as is evident in Fig. 1, having a threshold at $V \sim -20$ or −10 mV. The time constant of activation near threshold was relatively large, as illustrated by the −10 mV record in Fig. 1. At more positive potentials, the activation rate increased. Moreover, the amplitude of the time-dependent current decreased with depolarization and was essentially nil at $V \sim +30$ mV. Time-dependent deactivation or "tail" currents were also observed after return to the holding potential. The amplitude of these results reached a saturating level with a step potential of ~+30 mV.

Further information concerning the kinetics of the time-dependent component (I_{Kr}) was obtained with negative going steps to various different potentials after a prepulse of 2 s duration to +40 mV, as illustrated in Fig. 2. Several records elicited by the second voltage step, V_2 (upper inset of Fig. 2), are shown superimposed. These results may appear out of sequence, because the steady-state current at the end of the $V_2 = -45$ and −55 mV records lies above that of the $V_2 = 0$ and −35 mV records, largely because of I_{K1}. Similarly, the steady-state current at the end of the −65 and −75 mV results lies below that of the −55 mV record, because this voltage range is on the positive slope portion of

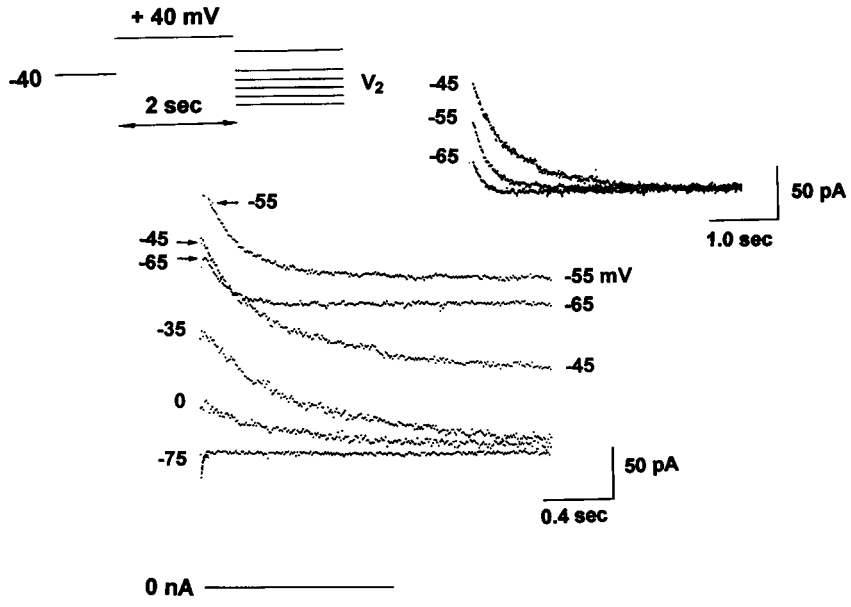

FIGURE 2 Membrane currents elicited by steps to the potentials indicated (V_2) after a 2-s duration step to +40 mV (V_1). The protocol is illustrated in the upper left inset. A 4-s rest interval was used between each application of the two-step sequence. The zero current level is indicated by the 0 nA line below these results. The −45, −55, and −65 mV results are shown in the upper right inset with the steady-state current subtracted.

the I_{K1} current-voltage relation. As an aid to better visualization of these results, the −45, −55, and −65 mV records are illustrated on a longer time scale in the upper right inset of Fig. 2 with the steady-state component removed.

The time-dependent currents illustrated in Fig. 2 were well described by single exponential functions of time, as shown in Fig. 3. The steady-state current obtained at the end of 4 s (the duration of V_2 in the two-step protocol illustrated in Fig. 2) was subtracted from each of these records, as with the results in the inset of Fig. 2, and the remaining current was plotted semilogarithmically. The time constants obtained from this analysis from several preparations (n = 6) are represented in Fig. 4 *A*. (The results for V = 10 and 20 mV in Fig. 4 *A* were obtained from activation kinetics, such as those illustrated in Fig. 1.) A notable feature of these results is the relatively large values of the time constant over a fairly broad range of potentials, with a maxium of ~0.8 s at $V \approx -30$ mV. The tail current amplitude as a function of

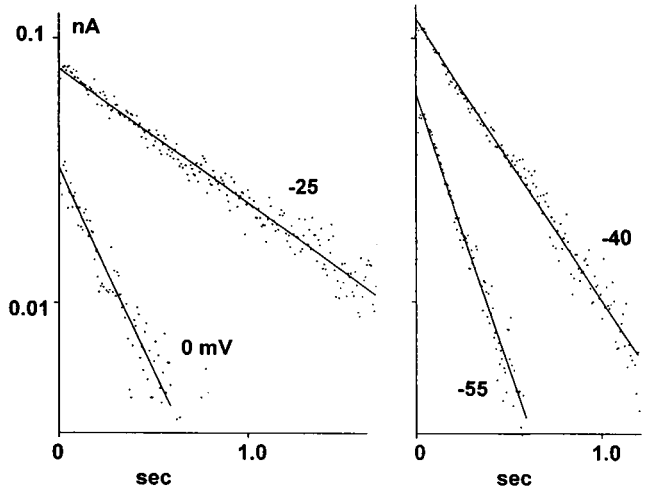

FIGURE 3 Semilogarithmic plots of time-dependent currents from the preparation illustrated in Fig. 2. Potentials of the second step (V_2) in the two-step protocol are as indicated. Straight lines are least-squares best fits to these results.

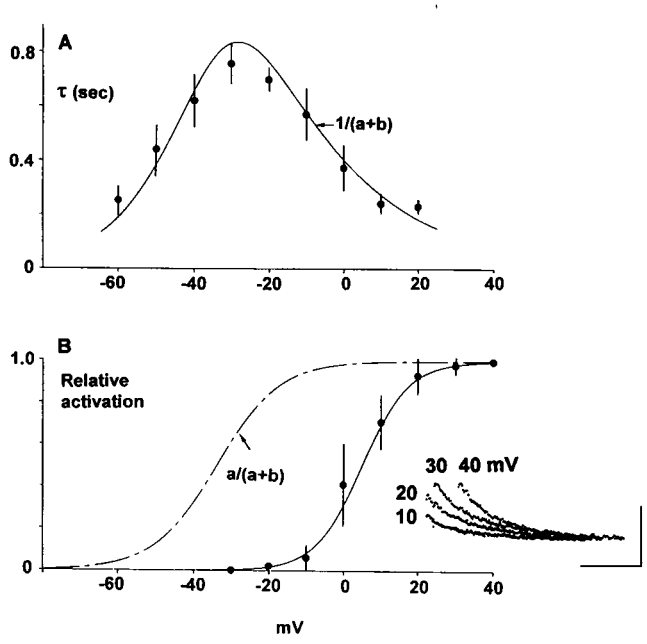

FIGURE 4 (*A*) Time constants as obtained by the procedure illustrated in Fig. 3. The error bars indicate mean ± SD (n = 6). The bell-shaped curve labeled $1/(a + b)$ corresponds to $a = 0.9 \exp(0.04(V + 25))\ s^{-1}$ and $b = 0.31 \exp(0.08(V + 25))\ s^{-1}$. (*B*) Steady-state activation curve obtained from normalization of tail currents at −40 mV after steps to potentials indicated on the abscissa. An illustration of these results is given in the inset (calibrations are 0.5 s and 0.1 nA). The maximum, saturating tail current amplitude was used to normalize tail currents for all voltage steps. The results of this procedure for six preparations are shown. The dashed curve corresponds to $(a + b)^{-1}$, where a and b are given in (*A*). The solid curve corresponds to $(1 + \exp(0.0017(V - 5)))^{-1}$.

step potential from experiments such as those in Fig. 1 is shown in Fig. 4 *B* normalized to the maximum, saturating tail current amplitude for each experiment. (An illustration of the saturation of tail current amplitude as a function of step potential is illustrated in the inset of Fig. 4 *B*.)

We have described the results in Fig. 4 by a closed-open gating model represented by [C] $\underset{b}{\overset{a}{\rightleftarrows}}$ [O], where [C] and [O] are the closed and open states of the channel, respectively, and a and b are the activation and deactivation rate constants, respectively. The time constant of the macroscopic current of this model is given by $(a + b)^{-1}$, and steady-state activation is given by $a/(a + b)$. The parameters a and b, which are voltage dependent, are represented in the model by $a_o \exp(a_1(V - V_o))$ and $b_o \exp(-b_1(V - V_o))$, respectively (Stevens, 1978). The various parameters in a and b were chosen so as to fit, by eye, the kinetic results in Fig. 4 *A*. The activation curve, $a/(a + b)$, is represented by the dashed line in Fig. 4 *B*. The model clearly does not provide a reasonable description of the experimentally determined activation results. Conversely, if a and b were modified so as to fit the results in Fig. 4 *B*, then the model would not accurately describe the kinetics. Consequently, the results in Fig. 4, *A* and *B*, taken together, comprise a gating model paradox (see Discussion). The theoretical description of the results in Fig. 4 *B* (solid line) is the Boltzmann distribution, $(1 + \exp(zq(V + V_{1/2})/kT)^{-1}$, with $z = 4$ and $V_{1/2} = 5$ mV, and q, k, T all with their usual meaning ($kT/q = 26.3$ mV at $T = 34$°C). This relation does not have an obvious interpretation in terms of gating kinetics.

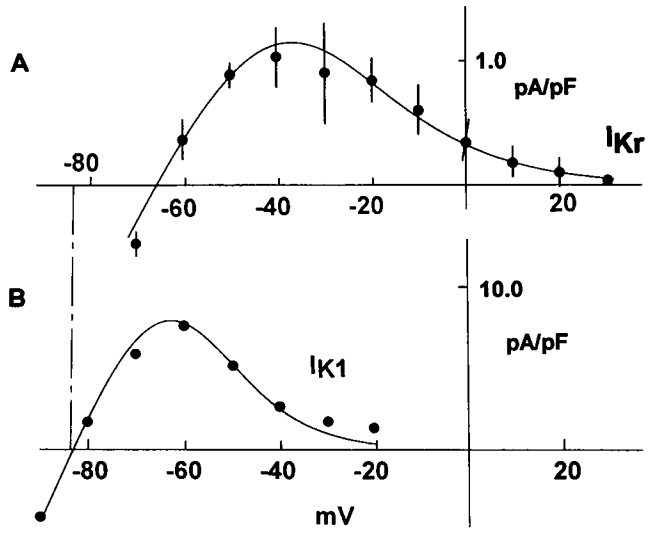

FIGURE 5 (*A*) Fully activated current-voltage relation for I_{Kr}. The results for $V < -20$ mV correspond directly to amplitudes of tail currents after a 2-s prepulse to +40 mV, such as the results shown in Fig. 2. The $-20 \leq V \leq 0$ mV range of this relation was also determined from tail current amplitudes corrected for the fact that the channel does not fully deactivate in this potential range (*B*). That is, the tail current in this range was divided by $(1 - n_\infty)$, where n_∞ corresponds to the relative activation of the channel at the potential at which the tail current was measured in the −20 to 0 mV range. The $V > +10$ mV portion of this relation was obtained from the on-off ratio procedure of Noble and Tsien (1968), as indicated in the text. The error bars indicate mean ± SD ($n = 3$). The solid line represents $66(V + 66)/(1 + 0.08 \exp(0.075(V + 66)))$ pA/pF. (*B*) Representative current-voltage relation for background current (I_{K1}), as described in the text. The solid line represents $670(V + 83)/(1 + .06 \exp(.12(V + 83)))$ pA/pF. The dashed line illustrates the difference between the reversal potentials for I_{K1} and I_{Kr}, as described in the text.

Fully activated current voltage relation

The fully activated current voltage relation for the time-dependent component illustrated in Figs. 1–3 is shown in Fig. 5 *A*. The results for $V \leq 0$ mV were obtained from tail current amplitudes such as those in Fig. 2 with the appropriate corrections for the observation that the channel does not fully deactivate in the steady state for $-20 \leq V \leq 0$ mV (Fig. 4 *B*). That is, a prepulse to +40 mV 2 s in duration is sufficient to fully activate the time-dependent conductance. A subsequent step to $V < -20$ mV results in complete deactivation of the conductance. Therefore, the time-dependent currents in Fig. 2 for $V < -20$ mV represent the fully activated amplitude of this component for these potentials. A slight correction in this procedure is required for $-20 \leq V \leq 0$ mV to account for incomplete deactivation of the conductance (Fig. 5, legend). The results in Fig. 5 *A* for $V \geq 10$ mV were obtained from the ratio procedure of Noble and Tsien (1968) from records such as those in Fig. 1. That is, the ratio of the time-dependent current activated by a step to these potentials was divided by the amplitude of the tail current upon return to the holding potential, and this ratio was then multiplied by the maximal, saturating amplitude of tail current obtained with step potentials to $V \geq +30$ mV. The final result in Fig. 5 *A* shows clear inward-going rectification with the fully activated current at ~0 for $V \geq +30$ mV. By comparison, the current-voltage relation of the background current is illustrated in Fig. 5 *B*. This result was obtained from the steady-state current at the end of the 4-s V_2 step of the two-step protocol given in Fig. 2. We attribute this result to I_{K1}, especially for $V < -40$ mV. The slope of this relation is negative for $V > -40$ mV, but a second, time-independent component does appear to contribute in this potential range, as noted above. The theoretical curves in Fig. 5 are ad hoc descriptions of inward rectification given by $a(V - E_{rev})/(1 + b \exp(c(V - E_{rev}))$, where $a = 66.0$ pS/pF, $b = 0.08$, $c = 0.075$ mV^{-1}, and $E_{rev} = -66$ mV for Fig. 5 *A*, and $a = 670.0$ pS/pF, $b = 0.06$, $c = 0.12$ mV^{-1}, and $E_{rev} = -83$ mV for Fig. 5 *B*.

A significant aspect of the above analysis is the difference between the reversal potential for the time-dependent conductance and I_{K1}, as indicated by the dashed line in Fig. 5. This result is also apparent in the −75 mV record in Fig. 2. The I_{Kr} component is clearly inward at this potential, which demonstrates that the I_{Kr} reversal potential is positive to −75 mV. However, the steady-state current at the end of this record, which we attribute to I_{K1}, is outward, which indicates that E_{rev} for I_{K1} is negative to −75 mV. We determined the reversal potential for I_{Kr} from interpolation of time-dependent currents (e.g., the −75 and −70 mV

records (the latter not shown) for the experiment described in Fig. 2). Similarly, the reversal potential for I_{K1} was determined from interpolation of the steady-state currents at the end of the second voltage step in the protocol illustrated in Fig. 2. Pooled results for E_{rev} with 5 mM K_o are −84.6 ± 4.9 mV for I_{K1} and −70.3 ± 4.4 mV for the time-dependent component (n = 6; mean ± SD), as shown in Fig. 6. The difference between the results for E_{rev} based on measurements from the same preparations was 16.4 ± 7.1 mV. Also shown in Fig. 6 are results with K_o = 2.5, 10, and 15 mM. The difference in E_{rev} for these conditions was 21.0 ± 7.6 mV, 13.9 ± 8.2 mV, and 11 mV (average from two preparations), respectively. The straight line in Fig. 6 has a slope of 54.6 ± 6.9 mV per decade of K_o, as determined from least-squares regression, which is consistent with the background current (I_{K1}) being a potassium selective conductance, as shown previously (Sakmann and Trube, 1984; Harvey and Ten Eick, 1988). The results for the time-dependent component suggest that this current is also carried at least in part by potassium ions, but the deviation of the reversal potential from the potassium ion equilibrium potential, E_K, especially for low levels of K_o, suggests that another ion, possibly sodium, also permeates this channel. This effect is modeled by the curved line in Fig. 6, which is given by $E_{rev} = -kT/q \ln(K_i/(K_o + \gamma Na_o))$ with $\gamma = 0.04$ and the various ion concentrations as given in Fig. 6. That is, external sodium ions appear to permeate the I_{Kr} channel about 4% as effectively as external potassium ions.

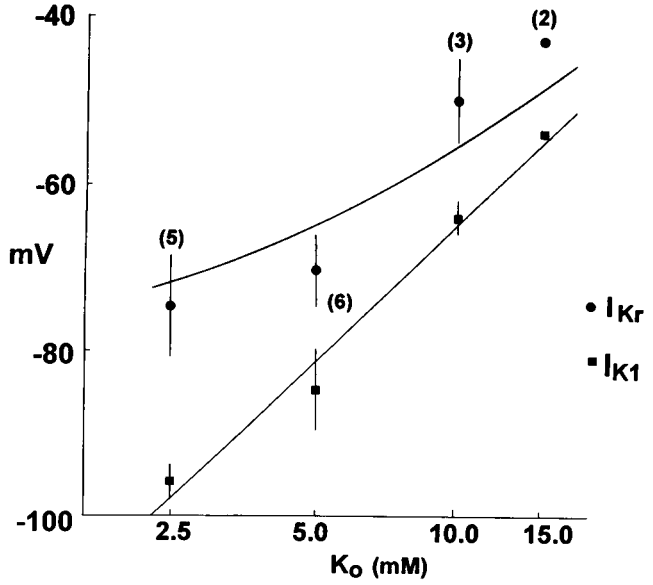

FIGURE 6 Reversal potential measurements for I_{K1} and I_{Kr} as a function of external potassium ion concentration (K_o). The numbers above each set of results indicates the number of experiments for each level of K_o. The error bars indicate ± SD. The slope of the straight line through the I_{K1} results is 54.6 mV per decade change in K_o. The curved line corresponds to $-54.6 \log(K_i/(K_o + \gamma Na_o))$, where K_o is given by the abscissa, Na_o = 121 mM, K_o = 140 mM, and γ = 0.04.

Block of I_{Kr} by E-4031

The effects of E-4031 (1 μM), both on the action potential (AP) waveform and on membrane current, are illustrated in Fig. 7. The action potentials illustrated in Fig. 7 were obtained by suprathreshold current stimuli (pulse duration = 5 ms; stimulus rate = 1 Hz) in controls and after the addition of E-4031 to the external solution. The drug increased the duration of the AP, as noted previously (Jurkiewicz and Sanguinetti, 1993; Veldkamp et al., 1993), and it blocked I_{Kr} as shown in the inset of Fig. 7. The block of I_{Kr} produced by 1 μM E-4031 was complete at all potentials (n = 5). In other words, the time-dependent currents observed in these experiments are attributable solely to I_{Kr}.

DISCUSSION

This paper describes novel measurements of the E-4031-sensitive repolarization current (I_{Kr}) in a mammalian cardiac ventricular myocyte preparation. One striking result concerns the amplitude of the kinetics of this component. We found that I_{Kr} has a time constant of ~0.6 to 0.8 s over a fairly broad voltage range (−40 to −10 mV), in contrast to the original measurements of Sanguinetti and Jurkiewicz (1990), who found a maximum time constant for I_{Kr} in guinea pig ventricular myocytes of only 0.18 s. Recently, Yang et al. (1994) reported an I_{Kr} component from atrial tumor myocytes derived from transgenic mice having a maximum time constant of ~0.7 s. However, their results were obtained at room temperature. An extrapolation of their results to 35°C with a Q_{10} of 3 suggests that the I_{Kr} component in these cells is probably similar to that of guinea pig ventricular myocytes. As noted below, our results compare favorably with measurements of the E-4031-sensitive component in cat ventricular myocytes by Follmer et al. (1992), which raises the possibility that I_{Kr} in mam-

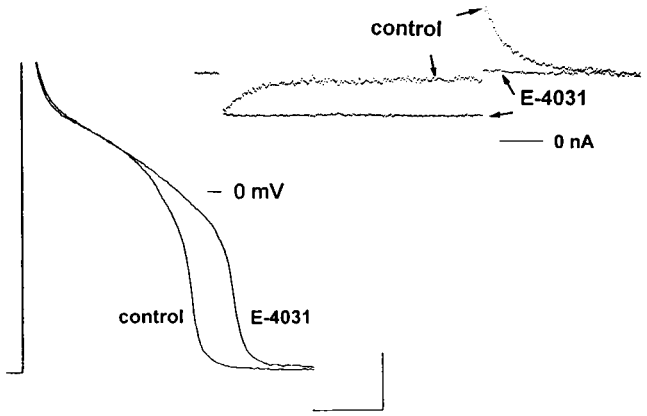

FIGURE 7 Effects of E-4031 (1 μM) on the action potential waveform and on membrane current. (*Inset*) holding potential = −40 mV; step potential = +20 mV. The calibrations represent 100 ms and 25 mV for the action potentials, and 0.5 s and 0.1 nA for the membrane current results in the inset.

malian preparations has two (or more) isoforms, one that corresponds to cat and rabbit hearts, and another for guinea pig hearts. The obvious question arising from this comparison is: Which isoform is present in humans? This is a question that can be answered only by experiments on human cardiac cells. The recent work by Wang et al. (1994) on single myocytes isolated from human right atrial appendages appears to suggest that the E-4031 component in humans is rapid, as in the guinea pig results of Sanguinetti and Jurkiewicz (1990). However, further experiments will be needed to comfirm this point. A human potassium ion channel, HERG, has recently been cloned which has kinetic properties similiar to those of I_{Kr}, as determined from heterologous expression in *Xenopus* oocytes (Sanguinetti et al., 1995), but a detailed, quantitative comparison between our results and the HERG results is difficult to carry out because of differences in expression system (oocytes vs. cardiac myocytes) and in the temperature used for recordings. Moreover, the currents expressed in oocytes were not blocked by E-4031, which further indicates that more work is needed with heterologous expression of I_{Kr} before a comparative analysis of these results with measurements of I_{Kr} in native cells can be carried out. One intriguing aspect of the work by Sanguinetti et al. (1995) in the context of this study is that they found a maximum time constant of ~2 s for HERG at room temperature, which, with a Q_{10} of 3, would correspond with the maximum time constant of 0.7 s in our work and in the results of Follmer et al. (1992) for T = 33–35°C.

A gating model paradox

In their original work on E-4031-sensitive current, Sanguinetti and Jurkiewicz (1990) also presented a partial mathematical description of their results. In particular, they described the activation curve of I_{Kr} with a Boltzmann distribution which, however, does not yield insight concerning gating kinetics. In any gating model approach, channel activation and kinetics are fundamentally linked. For example, the kinetic results of Sanguinetti and Jurkiewicz (1990, their figure 11C) are very well described in the simple closed-open gating scheme given above (see Results) by $\tau = (a + b)^{-1}$ with $a = 2.8 \exp(0.055(V + 35))\ s^{-1}$ and $b = 2.8 \exp(-0.06(V + 35))\ s^{-1}$. However, the activation curve of the model, i.e., $a/(a + b)$, does not correspond very well to experiment (figure 9 of Sanguinetti and Jurkiewicz, 1990). The midpoint of the theoretical curve is −37 mV as compared to the experimental result of −22 mV, and the slope of the curve at its midpoint is only half as steep as the experimental result. These discrepancies between the closed-open state model and experimental results are even more apparent in this study. The simple gating scheme would appear to be appropriate for our results given that the activation and deactivation kinetics are both well described by single exponential functions of time. However, we cannot rule out the presence of a very rapid inactivation process that may contribute to inward rectification of the channel. Indeed, Shibasaki (1987) reported such a mechanism in a repolarization current from rabbit nodal cells that has properties similiar to those of I_{Kr}. In particular, those results provide clear evidence for rapid inactivation in whole cell recordings during depolarizing voltage steps, an effect that we have not observed, and a rapid removal of inactivation, as evidenced by a "hook" in deactivation, or "tail" currents, which may be present in some of our results. Moreover, Veldkamp et al. (1993) clearly observed a "hook" in single-channel recordings of tail currents of I_{Kr} in rabbit ventricular myocytes at room temperature. A rapid inactivation process at depolarized potentials and a concomitant, rapid removal of inactivation at potentials below the activation range of I_{Kr} can alter the relationship between channel activation and the slow kinetics of the gating apparatus. For example, one gating scheme that incorporates both processes is given by

$$[C] \underset{b}{\overset{a}{\rightleftharpoons}} [O] \underset{\lambda}{\overset{\kappa}{\rightleftharpoons}} [I]$$

where [C] and [O] are the closed and open states of the channels, respectively, as described above, and [I] is the inactivated state of the channel. In this scheme the channel must first open before the channel can inactivate and, conversely, it must leave the inactivated state before the channel can close. The model can readily account for a "hook" in tail currents when κ and λ are both significantly larger than a and b. Moreover, the envelope of tail current amplitudes at −40 mV, for example, is once again given by $a/(a + b)$. Furthermore, the tail current time constant is given by $[(\kappa + \lambda)/\lambda]\tau$, with $\tau = (a + b)^{-1}$ (Clay, 1985). That is, the tail current time constant at −40 mV, for example, is increased relative to the prediction of the simple open-close gating scheme by the degree of inactivation at −40 mV. However, the degree of inactivation in steady-state conditions at −40 mV is not very significant. The I_{Kr} component is absent in voltage steps in the −40 to −20 mV range with a holding potential of −40 mV not because of inactivation, but because this voltage range lies below the activation range of the channel. Consequently, the closed-open inactivated state model does not significantly alter the relationship between activation and the bell-shaped curve that describes the kinetics. The voltage dependencies of a and b can be chosen so as to fit the activation curve in Fig. 4 *B*. However, the model fails to fit the time constant results, even with the expression for τ given above. For example, $(\lambda + \kappa)/\lambda$ would be equal to ~1.5 at −40 mV, if the rectification of I_{Kr} were due entirely to inactivation (Fig. 5 *A*), whereas this ratio would have to be ~100 at this potential if the model were to describe the voltage dependence of I_{Kr} kinetics. The gating paradox apparently remains. An I_{Ks} component has recently been described in rabbit ventricular myocytes by Salata et al. (1995), which might suggest that the paradox is due in some way to this current. However, the time-dependent currents in this study were blocked by E-4031, as demonstrated in Fig. 7, which

argues against this possibility. Moreover, the paradox is apparent even in the original measurements of I_{Kr} from guinea pig ventricular myocytes of Sanguinetti and Jurkiewicz (1990), as noted above, in which a large I_{Ks} component is clearly present. An alternative approach to the problem might be two voltage sensors, one that determines activation of the conductance, and another that determines kinetics. However, attempts to model our results with a mechanism of this type were unsuccessful, primarily because channel activation and channel kinetics are fundamentally linked, as previously noted. A somewhat similar situation applies to the Hodgkin and Huxley (1952) model of I_K in nerve. The maximum time constant in that model occurs at $V \approx -60$ mV, which is at the foot of the activation curve. However, I_K in nerve has a sigmoidal time-dependent activation, which is represented in the Hodgkin and Huxley (1952) model by raising the activation parameter to the fourth power. This procedure effectively shifts the midpoint of the activation curve rightward along the voltage axis and steepens the voltage dependence of the curve. A similar situation does not appear to apply to our results, inasmuch as we have not observed a clear delay, i.e., sigmoidal activation of I_{Kr}. The delay should be clearly observable for a model similar to that of Hodgkin and Huxley (1952) to apply in this case.

Comparison with other preparations

The E-4031-sensitive repolarization current in rabbit ventricular myocytes is activated at relatively positive membrane potentials (Fig. 4 *B*). This result compares favorably with the single channel recordings by Veldkamp et al. (1993), and it is similar to the results from cat ventricular myocytes of Follmer et al. (1992). We used a relatively positive holding potential, −40 mV, for our experiments, which Follmer et al. (1992) have demonstrated has no effect on I_{Kr}, provided the holding potential lies below the threshold for activation of this component. By contrast, the activation curves for I_{Kr} in guinea pig ventricular myocytes and in chick atrial heart cell aggregates lie at relatively more negative potentials, having midpoints of −22 and −36 mV, respectively (Sanguinetti and Jurkewicz, 1990; Shrier and Clay, 1986; Shrier et al., unpublished observations). As noted above, further differences regarding this component in the various preparations in which it has been observed concern the magnitude of its kinetics. The maximum time constant of I_{Kr} in the chick heart cell preparation is ~1 s at 36°C, which is about the same that of I_{Ks} in this preparation (Shrier and Clay, 1986; Clay et al., 1988). The time constants of this component reported here for rabbit heart cells are also relatively large, having a maximum of 0.8 s (34°C), and the kinetic results in Follmer et al. (1992) also appear to be consistent with our observations. Specifically, the time constant at −30 mV in their recordings is ~0.7 s (figure 7A of Follmer et al., 1992). If this result corresponds to the maximum time constant for I_{Kr} in cat ventricular myoctyes, then the paradox we have described above also applies in this preparation, because the midpoint of activation is ~+10 mV (Follmer et al., 1992). By contrast, the kinetics of I_{Kr} in guinea pig ventricular myocytes are, indeed, considerably faster than those of I_{Ks}, which justifies the terminology I_{Kr} ("r" for rapid) in that preparation.

A further, significant comparison between these results and previous work concerns the reversal potential of the E-4031-sensitive component. In both chick and guinea pig heart cells it appears to be selective only to potassium ions (Shrier and Clay, 1986; Sanguinetti and Jurkiewicz, 1990). By contrast, the I_{Kr} reversal potential in this study in physiological saline is ~15 mV positive to that of I_{K1}, which is known to be a K^+ selective conductance (Sakmann and Trube, 1984; Harvey and Ten Eick, 1988) (Fig. 6). The results given here for E_{rev} are reminiscent of the original I_{x1} analysis of Noble and Tsien (1969), who reported a time-dependent outward current activated at depolarized potentials in cardiac Purkinje fibers, which reversed at a potential that was 10–20 mV positive to E_K. Indeed, this result prompted the "x" terminology, because the ionic constitutent(s) of the current component were unknown. Similarly, the ionic constituents of the E-4031-sensitive component in rabbit heart cells must be considered at this point to be an unresolved issue, although the conductance would appear to be carried at least in part by potassium ions (Fig. 6). The observation that E_{rev} for I_{Kr} is 15–20 mV positive to the resting potential suggests that this component might actually contribute *inward* current during the latter part of phase 3 of the action potential, although the rapid deactivation kinetics of the current for $V < -60$ mV suggest that this effect is relatively minor.

The significance of I_{Kr} is that it appears to play a role in antiarrhythmic drug therapy, inasmuch as E-4031, dofetilide, and amokalant have marked antiarrhythmic and proarrhythmic effects on the heart, apparently because of blockade of I_{Kr} (Sasyniuk and Carmeliet, 1995). This component contributes to repolarization, as illustrated by the action potential recordings in Fig. 7. The early part of the plateau phase is unaffected by E-4031, which is consistent with the rectification of the I_{Kr} open-channel *IV* relation in Fig. 5 *A*. That is, even though the I_{Kr} channel gate is fully, or almost fully, activated during the plateau phase, very little current flows through the channel because of its intrinsic rectification properties. As the membrane potential repolarizes, it essentially "scans" the *IV* curve, because the I_{Kr} gate does not have time to close before repolarization is complete, especially since the range of its maximal time constants occurs in the voltage range ($-60 < V < 0$ mV), where it has its maximum effect on the action potential. The role of I_{Kr} kinetics in normal and abnormal functioning of the heart is less clear, as, indeed, is the mechanism by which blockade of the current leads to antiarrhythmic action. These issues await further study.

We gratefully acknowledge excellent technical assistance from Cedric Gordon and Kelly Harrison.

This work was supported by grants from the Medical Research Council, Canada (B.I.S. and A.S.) and a grant from the Québec Heart Foundation (B.I.S.). A.O. was partially supported by a stipend from FRSQ-(Subvention d'équipe en pharmacologie-pharmaceutique) (B.I.S.). T.P. was supported by a stipend from Fonds pour la formacion de Cherchers et l'Aide à la Recherche.

REFERENCES

Bennett, P. B., L. C. McKinney, R. S. Kass, and T. Begenisich. 1985. Delayed rectification in the calf cardiac Purkinje fiber. Evidence for multiple state kinetics. *Biophys. J.* 48:553–567.

Carmeliet, E. 1992. Voltage- and time-dependent block of the delayed K^+ current in cardiac myocytes by dofetilide. *J. Pharm. Exp. Ther.* 262: 809–817.

Carmeliet, E. 1993. Use-dependent block and use-dependent unblock of delayed rectifier K^+ current by amokalant in rabbit ventricular myocytes. *Circ. Res.* 73:857–868.

Clay, J. R. 1985. Comparison of the effects of internal TEA^+ and Cs^+ on potassium current in squid giant axons. *Biophys. J.* 48:885–892.

Clay, J. R., C. E. Hill, D. Roitman, and A. Shrier. 1988. Repolarization current in embryonic chick atrial heart cells. *J. Physiol.* 403:525–537.

Coraboeuf, E., and E. Cameliet. 1982. Existence of two transient outward currents in sheep Purkinje fibres. *Pflugers Arch.* 392:352–359.

Duan, D-Y., B. Fermini, and S. Nattel. 1992. Sustained outward current observed after I_{to1} inactivation in rabbit atrial myocytes is a novel Cl^- current. *Am. J. Physiol.* 262:H1967–H1971.

Follmer, C. H., and T. J. Colatsky. 1990. Block of delayed rectifier potassium current, I_K, by flecainide and E-4031 in cat ventricular myocytes. *Circulation.* 82:284–293.

Follmer, C. H., N. J. Lodge, C. A. Cullinan, and T. J. Coltasky. 1992. Modulation of the delayed rectifer, I_K, by cadmium in cat ventricular myocytes. *Am. J. Physiol.* 262: C75-C83.

Giles, W. R., and A. C. G. van Ginneken. 1985. A transient outward current in isolated cells from the crista terminalis of rabbit heart. *J. Physiol.* 368:243–264.

Hamill, O. P., A. Marty, E. Neher, B. Sakmann, and F. Sigworth. 1981. Improved patch-clamp techniques for high-resolution current recording from cells and cell-free membrane patches. *Pflugers Arch.* 391:85–100.

Harvey, R. D., and J. R. Hume. 1989. Isoproterenol activates a chloride current, not the transient outward current, in rabbit ventricular myocytes. *Am. J. Physiol.* 257:C1177–C1181.

Harvey, R. D., and R. E. Ten Eick. 1988. Characterization of the inward-rectifying potassium current in cat ventricular myocytes. *J. Gen. Physiol.* 91:593- 615.

Hodgkin, A. L., and A. F. Huxley. 1952. A quantitative description of membrane current and its application to conduction and excitation in nerve. *J. Physiol.* 117:500–544.

Isenberg, G., and U. Klockner. 1982. Calcium tolerant ventricular myocytes prepared by preincubation in a "KB medium." *Pflugers Arch.* 395:6–18.

Josephson, I. R., J. Sanchez-Chapula, J., and A. M. Brown. 1984. Early outward current in rat single ventricular cells. *Circ. Res.* 54:157–162.

Jurkiewicz, N. K., and M. C. Sanguinetti. 1993. Rate dependent prolongation of cardiac action potentials by a methanesulfamilide agent. Specific block of rapidly activating delayed rectifier K^+ current by dofetilide. *Circ. Res.* 72:75–83.

Matsuura, H., T. Ehara, and Y. Imoto. 1987. An analysis of the delayed outward current in single ventricular cells of the guinea-pig. *Pflugers Arch.* 410:596–603.

McDonald, T. F., and W. Trautwein. 1978. The potassium current underlying delayed rectification in cat ventricular muscle. *J. Physiol.* 274: 217–246.

Mitra, R., and M. Morad. 1985. A uniform enzymatic method for dissociation of myocytes from hearts and stomachs of vertebrates. *Am. J. Physiol.* 249:H1056–H1060.

Noble, D., and R. W. Tsien. 1968. The kinetics and rectifier properties of the slow potassium current in cardiac Purkinje fibers. *J. Physiol.* 195: 185–214.

Noble, D., and R. W. Tsien. 1969. Outward membrane currents activated in the plateau range of potentials in cardiac Purkinje fibres. *J. Physiol.* 200:205–231.

Ogbaghebriel, A., and A. Shrier. 1994. Inhibition of metabolism abolishes transient outward current in rabbit atrial myocytes. *Am. J. Physiol.* 266:H182–H190.

Sakmann, B., and G. Trube. 1984. Conductance properties of single inwardly rectifying potassium channels in ventricular cells from guinea-pig heart. *J. Physiol.* 347:641–657.

Salata, J. J., N. K. Jurkiewicz, B. Jow, P. J. Guinosso Jr., and B Fermini. 1995. Evidence for the slowly activating component of the delayed rectifier K^+ current (I_{Ks}) in rabbit ventricular myocytes. *Biophys. J.* 68:a147.

Sanguinetti, M. C., C. Jiang, M. E. Curran, and M. T. Keating. 1995. A mechanistic link between an inherited and an acquired cardiac arrhythmia: HERG encodes the I_{Kr} potassium channel. *Cell.* 81: 299–307.

Sanguinetti, M. C., and N. K. Jurkiewicz. 1990. Two components of cardiac delayed rectifier K^+ current. Differential sensitivity to block by class III antiarrhythmic agents. *J. Gen. Physiol.* 96:195–215.

Sasyniuk, B. I., and E. Carmeliet. 1995. Role of potassium channel modulators in the treatment of cardiac arrhythmias. *In* Pharmacological Science: Perspectives for Research and Therapy in the Late 1990s. A. C. Cuello and B. Collier, editors. Birkhausen, Basel. 335–346.

Shibasaki, T. 1987. Conductance and kinetics of delayed rectifier potassium channels in nodal cells of the rabbit heart. *J. Physiol.* 387:227–250.

Shrier, A., and J. R. Clay. 1986. Repolarization currents in embryonic chick atrial heart cell aggregates. *Biophys. J.* 50:861–874.

Stevens, C. F. 1978. Interactions between membrane-protein and electric field. Approach to studying nerve excitability. *Biophys. J.* 22:295–306.

Veldkamp, M. W., A. C. G. van Ginneken, and L. N. Bouman. 1993. Single delayed rectifier channels in the membrane of rabbit ventricular myocytes. *Circ. Res.* 72:865–878.

Wang, Z., B. Fermini, and S. Nattel. 1994. Rapid and slow components of delayed rectifier current in human atrial myocytes. *Cardovasc. Res.* 28:1540–1546.

Yang, T., M. S. Wathen, A. Felipe, M. M. Tamkun, D. J. Snyders, and D. M. Roden. 1994. K^+ currents and K^+ channel mRNA in cultured atrial cardiac myocytes (AT-1 Cells). *Circ. Res.* 75:870–878.